Electronic States of Alkanethiolate Self-Assembled Monolayers on Au(111) Studied by Two-Photon Photoemission Spectroscopy

ARTICLE *in* THE JOURNAL OF PHYSICAL CHEMISTRY C · JUNE 2012

Impact Factor: 4.77 · DOI: 10.1021/jp302545r

4 AUTHORS, INCLUDING:

Masahiro Shibuta
Keio University
20 PUBLICATIONS **95** CITATIONS

SEE PROFILE

THE JOURNAL OF PHYSICAL CHEMISTRY C

Article

pubs.acs.org/JPCC

Electronic States of Alkanethiolate Self-Assembled Monolayers on Au(111) Studied by Two-Photon Photoemission Spectroscopy

Naoyuki Hirata,[†] Masahiro Shibuta,[†,‡] Ryo Matsui,[†] and Atsushi Nakajima*[,†,‡]

[†]Department of Chemistry, Faculty of Science and Technology, Keio University, 3-14-1 Hiyoshi, Kohoku-ku, Yokohama 223-8522, Japan

[‡]JST, ERATO, Nakajima Designer Nanocluster Assembly Project, 3-2-1 Sakado, Takatsu-ku, Kawasaki 213-0012, Japan

ABSTRACT: Two-photon photoemission (2PPE) spectroscopy has been employed to probe the electronic states of *n*-alkanethiolate self-assembled monolayers (SAMs) on an Au(111) substrate fabricated in a wet chemical process. Electronic states newly formed in the SAM formation were observed below and above the Fermi level (E_F) for various alkyl chain lengths of C12-, C18-, and C22-SAMs. At 3.5−3.7 eV above E_F, an unoccupied state originating from a bond between gold and sulfur atoms appears, a state that shows little dispersion with parallel to the surface. The peak position of the unoccupied state depends on the substrate temperature, and it was stabilized with increasing temperature; E_F +3.7 eV at 85 K and E_F +3.5 eV at 330 K for C18-SAM. The stabilization of the state is attributed to the increase of intermolecular interaction at sulfur atoms with their neighboring S atoms, which is caused by a change in the tilt angle of the alkyl chains in the SAM: on increasing the temperature, the interaction between S atoms in the SAM is promoted by the more upright alkyl chains.

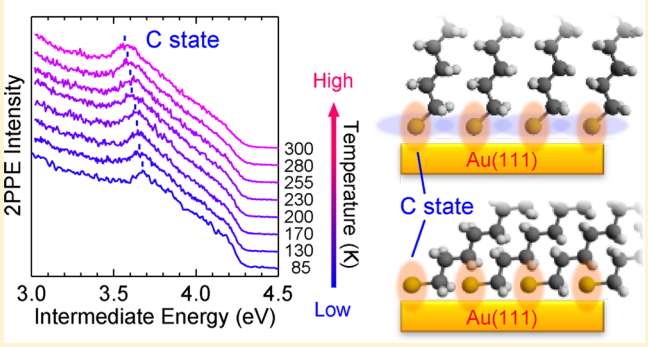

1. INTRODUCTION

In the past decades, designing surface properties by creating functionalized molecular layers on a substrate has been the subject of many investigations. In particular, the use of a self-assembled monolayer (SAM) has attracted considerable attention due to its many potential applications in such areas as sensors, corrosion inhibition, lithography, and molecular electronics.[1−6] The most widely studied SAM systems are *n*-alkanethiolate (C*n*-; *n* is the number of carbon atoms in the alkyl chains) SAMs on an Au(111) surface because highly ordered structures can be easily prepared that possess chemical and thermal stability.[7,8] The study of the geometric and electronic structures of such SAMs is important in order for us to be able to utilize them for various scientific and technological applications. In particular, a scientific understanding of adsorption-induced electronic states, formed by chemical interaction between a substrate and molecules, can reveal the mechanism of carrier transportation at the surface and/or the interface.

So far, molecular arrangement and self-assembly mechanisms of the C*n*-SAMs have been widely investigated by infrared reflection absorption spectroscopy (IRAS),[9−11] low-energy electron diffraction (LEED),[12,13] helium atom diffraction,[14] thermal desorption spectroscopy (TDS),[15] atomic force microscopy (AFM),[16,17] and scanning tunneling microscopy (STM).[10,15,18−21] The important insights obtained from these previous studies are: in the early stage of a self-assembly process, alkanethiolates on Au(111) are formed with the long alkyl chain parallel to the surface ($p \times \sqrt{3}$ structure), which is often referred to as the "lying-down" structure.[15,17,22] Then, after increasing the coverage of alkanethiolates to near saturation, the chains stand up with a tilt angle of ∼30° from the surface normal to form the $(\sqrt{3} \times \sqrt{3})R30°$ or $c(4 \times 2)$ super structure, usually called the "standing-up" structure.[15,17,22]

On the other hand, the electronic structures of SAM/Au(111) systems have not been investigated extensively. With regard to the occupied states, ultraviolet photoemission spectroscopy (UPS) and X-ray photoemission spectroscopy (XPS) have been performed to reveal the valence band structure below the Fermi level (E_F)[23] and to investigate the chemical environment of the emitting atom by analyzing core level shift,[24] respectively. However, the nature of the unoccupied states, which are significantly important for understanding the carrier dynamics at the interface, remains less clear. For their understanding, two-photon photoemission (2PPE) spectroscopy currently is a powerful tool to study the unoccupied states and electron dynamics for the metal or semiconductor surfaces including organic thin films. In the 2PPE process, an electron is pumped by a first photon from an occupied state to an unoccupied state, and then photoemission from the unoccupied state is induced by the second photon.[25]

Received: March 16, 2012
Revised: June 5, 2012
Published: June 15, 2012

   dx.doi.org/10.1021/jp302545r | *J. Phys. Chem. C* 2012, 116, 13623−13628

Therefore, both occupied and unoccupied electronic states can be probed by 2PPE at the same time. In the past 2PPE measurements for alkanethiolate SAMs, the chain length C*n*- has been limited to rather short (n = 4−12)[22,26,27] and the adsorption-induced electronic states below and above E_F were not fully resolved. Moreover, the correlation between electronic structures of SAM and thermo-dynamical change in the geometric structures has not been clarified, although it has been well recognized by IRAS and theoretical calculations.[9−11]

In the present study, we have performed 2PPE experiments for several chain length C*n*-SAM/Au(111) substrate systems (n = 12, 18, and 22) prepared in a wet chemical process where the geometric structure is well recognized as a "standing-up" structure in order to reveal the correlation between geometric and electronic structures of SAMs. We have fully observed the adsorption-induced occupied and unoccupied states derived from chemical interaction between the sulfur atom of the alkanethiolate molecule and the topmost gold (Au) atom. In addition, we have found that one of the unoccupied states is stabilized on increasing the temperature, reflecting a change in the geometrical conformations of the SAM.

2. EXPERIMENTAL SECTION

The experimental details of the preparation of C*n*-SAM/Au(111) substrate and 2PPE measurements have been described previously.[28−30] Briefly, an Au(111) single crystal (d = 10 mm, t = 1 mm, orientation accuracy of <0.1°, MaTecK corporation) was used as a substrate. The Au(111) surface was cleaned by repeated cycles of Ar^+ ion sputtering (0.6 kV, ∼1 μA, 15 min) and annealing (770 K, 30 min) in an ultrahigh vacuum (UHV) chamber. The surface cleanliness was confirmed by a 2PPE measurement (see Figure 1); the work function (WF) of 5.5 eV determined by the low-energy electron cutoff of the 2PPE spectrum and the sharp Shockley surface state (SS) located at 0.4 eV below E_F are both very sensitive to the flatness of the (111) surface and to the presence of surface defects.[27,31]

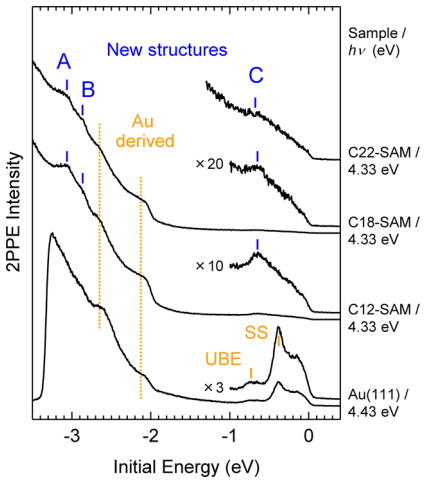

Figure 1. 2PPE spectra for the Au(111) clean surface and C12-, 18-, and 22-alkanethiolate SAMs/Au(111) surface measured with p-polarized light at 90 K. The photon energies are noted at the right-hand side. The horizontal axis indicates the initial energy related to E_F, and the high initial energy region of each 2PPE spectrum is magnified several times. Each peak position is marked by bars.

The SAM preparation was performed in air. The Au(111) substrate was first immersed into a piranha solution (3:1 concentrated H_2SO_4:H_2O_2) for about 20 min and then immersed into a 0.5 mM ethanolic solution of *n*-alkanethiol at room temperature (RT) for 20 h. The SAM sample was rinsed with pure ethanol and immediately introduced into the load lock chamber, and was allowed to dry sufficiently before it was transferred to the UHV chamber. Three different *n*-alkanethiol molecules (C12, C18, and C22) were used to examine the dependence on alkyl chain length. The surface uniformity of the C12-, C18-, and C22-SAMs was verified by STM measurement in UHV (see the Supporting Information in ref 30) and was in good agreement with known "standing-up" $(\sqrt{3} \times \sqrt{3})R30°$ or $c(4 \times 2)$ structures.[17,19−21] The surface contamination seemed negligible in our ex-situ preparation in solution.

All of the 2PPE experiments were performed in the UHV chamber with a base pressure of ∼1×10^{-8} Pa. As a light source, the third harmonics (4.04−4.77 eV, p-pol.) of a mode-locked Ti:sapphire laser (Coherent Mira 900, 780−920 nm, ∼100 fs pulse width, 76 MHz repetition rate) generated with a pair of β-BaB_2O_4 crystal were used. The light was focused onto the sample in the UHV chamber at an incident angle of 55° to the sample surface using an f = 400 mm concave mirror; the diameter of the spot size on the sample was up to 0.1 mm. The laser power was kept to be 0.13 nJ/pulse in order to avoid destruction of the SAMs and the influence of the space charge effect.[32] Note that all the 2PPE experiments were done with a single color, and thus, pump and probe pulses were not distinguished in this study. Photoelectrons emitted normal to the surface via two-photon processes were detected with a hemispherical electron energy analyzer (Thermo VG Scientific Alpha 110). The total energy resolution of the 2PPE setup was about 20 meV. In addition, angle-resolved (AR-) 2PPE measurements were performed to investigate the band dispersion of observed electronic states by rotating the sample. The sample temperature under 2PPE experiments was controlled between 85 and 330 K by liquid N_2 and by sample heating. The sample was biased at −1.00 V from the chamber ground, except for AR-2PPE measurements where the sample was grounded.

3. RESULTS AND DISCUSSION

3.1. 2PPE Spectra of SAM/Au(111). Figure 1 shows the monochromatic 2PPE spectra for the Au(111) clean surface (bottom) and C12-, C18-, and C22-SAMs on the Au(111) surface (upper) measured at 90 K. The horizontal axis indicates the initial energy relative to E_F. For the clean Au(111) surface, three characteristic structures were observed: (i) the structure at E_F −2.05 and −2.62 eV derived from the components of the 5d-band, (ii) the broad structure at E_F −0.8 eV derived from the upper band edge (UBE) of the sp-band, and (iii) the peak at E_F −0.4 eV derived from the SS. These findings were in agreement with published results.[27,31] The first image potential state (IPS) located at E_F +4.75 eV[33,34] cannot be accessed using a photon energy of 4.43 eV.

For the C12- and C18-SAMs, the two spectra seem quite similar to each other. It is reasonable that the electronic states are almost independent of the alkyl chain length. Instead of the SS and UBE features observed from a clean surface, the structure labeled by "C" was observed in the high initial energy region, as well as a rather smaller similar structure for C22-SAM. The intensity of the C structure was weakened as the

dx.doi.org/10.1021/jp302545r | J. Phys. Chem. C 2012, 116, 13623−13628

alkyl chain was lengthened, suggesting that the C state is localized near the gold (Au) and sulfur (S) bond. In addition to structure C, structures "A" and "B" were observed in the low initial energy region. The assignment and origin of these structures A and B are discussed in section 3.2. Interestingly, the intensities of two Au derived structures at E_F −2.05 and −2.62 eV remained even after forming SAMs, although such substrate-derived signals should be weakened by photoelectron scattering in the adsorbate. A considerable amount of intensity around the Au derived states implies that the adsorption induced electronic states are newly formed.[31,35−37] Indeed, adsorption-induced states mainly contributed by a metal orbital have been reported consistently; the photoemission enhancement around substrate-derived states was observed up to 1 ML.[37] The WF drastically decreased to be 4.25 ± 0.03 eV for all of the C*n*-SAM samples. As reported previously, the WF decrement is ascribed to the surface dipole layer on the Au(111) interface[23] and reconstruction of the Au(111) topmost layer on forming a SAM.[38]

3.2. Assignments of 2PPE Features. In order to identify whether the 2PPE peaks originate from occupied or unoccupied states, Figure 2a shows the photon energy dependence (4.13−4.33 eV) of the 2PPE spectra for the C18-SAM surface measured at 90 K. The horizontal axis indicates the intermediate energy relative to E_F; an unoccupied state should be fixed with constant intermediate energy. From the observed independence against the intermediate energies, structures A and C were assigned to be unoccupied states located at E_F +1.23 and +3.68 eV, respectively. On the other hand, structure B and the two Au-derived structures were shifted with photon energy. Since the amount of these shifts corresponds to the difference of one photon energy, structure B was assigned to be an occupied state located at E_F −2.83 eV; the energy position was determined by subtracting each photon energy from the intermediate energy. Figure 2b summarizes the energy levels observed in a C18-SAM/Au(111); unoccupied A and C states and occupied B and Au-derived states.

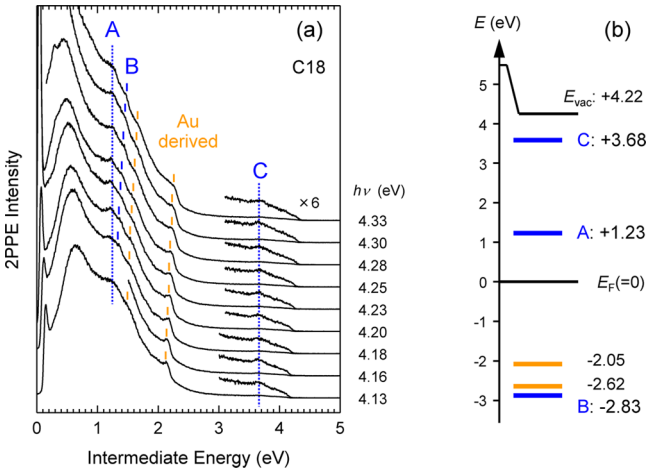

Figure 2. (a) Photon energy dependence of 2PPE spectra for a C18-SAM/Au(111) surface measured with p-polarized light at 90 K. The horizontal axis indicates the intermediate energy relative to E_F. Traces in the high intermediate energy region are magnified by 6 times. (b) The energy diagram of a C18-SAM/Au(111) surface obtained from the photon energy dependence of the 2PPE spectra.

We assigned the occupied B state as a localized bonding state between the topmost Au and S atoms, which is formed by the molecular adsorption of alkanethiol. Indeed, according to theoretical calculations, the highest occupied molecular orbital (HOMO) of alkanethiol molecules is mostly localized on the S atoms,[39] and in the adsorption, the HOMO is considerably coupled with the topmost Au atoms. Furthermore, a very similar occupied state with structure B was obtained by 2PPE for a low-coverage ("lying-down" structure) C4-SAM/Au(111) system.[27] For the UPS data for C18-SAM/Au(111), a structure has been consistently observed at an energy of E_F −2.5 eV,[40] although the intensity was very weak. The weakened occupied structure in the UPS result can be understood by the difference in probe depth of the experiments. The kinetic energy of photoelectrons excited by a He-I or He-II source used in the UPS measurements is several tens of eV which is around the minimum point of the universal curve.[41,42] On the other hand, the 2PPE measurement that detects a lower kinetic energy of photoelectrons (less than several eV) can more effectively probe buried and localized electronic states at a substrate−molecule interface, compared to the UPS.

Although the origin of the unoccupied structure A is not clear, it is likely that it is also an adsorption induced state arising from chemical Au−S bonding, because of the low density of state of a Au substrate and the wide HOMO−LUMO gap of an alkanethiol. Indeed, from the viewpoint of current−voltage (*I*−*V*) measurement based on STM, the electron conductance of the SAM is increased when the sample bias becomes around +1 V.[43] This result strongly supports that the unoccupied state is really located at that energy. Further theoretical studies may help to understand the origin of structure A.

3.3. Localized Character of the C State. The properties of the C state can be more easily discussed because, unlike the A and B states, there was little influence of secondary electrons. The energy position of the C state relative to the vacuum level (E_{vac}), that is, E_{vac} −0.55 eV, is close to the first IPS,[30,44] suggesting that it originates with the IPS formed on the SAM/Au(111). An AR-2PPE measurement can reveal whether the unoccupied state is localized or not with parallel to the surface.[44] Figure 3a shows the AR-2PPE result for the C state of C18-SAM at RT; little or no energy dispersion was observed over the whole range of emission angles. Moreover, the longer the alkyl chain, the less resolved became the C state (see Figure 1). The nondispersive and poorly resolved features of the C state show that it is largely localized at Au−S bonds. In fact, the localized state picture is in agreement with the dependence of the light polarization in 2PPE spectra (Figure 3b): the C state was observed even in s-polarized light which has the electric field vector parallel to the surface. This result also suggests that the C state is not an IPS because 2PPE from the IPS needs absolutely p-polarized light. Furthermore, the C state observation in s-polarization implies that the C state is characterized not by a pure σ-symmetry state between Au and S atoms but by a rather complicated interaction at the interface. A localized unoccupied state, similar to the C state, has been reported in the saturated phase of the C6-SAM/Au(111) system, while it was assigned to the σ^* antibonding orbital due to the chemical interaction between Au and S atoms.[22]

It should be noted that the IPS formed on the SAM can be observed when time-resolved (TR-) 2PPE, based on the pump−probe method, is used.[30] With a nonzero time delay, the IPS grew significantly and achieved a maximum intensity at about 4 ps, surprisingly surviving even at 200 ps after the pump pulse. The reason why the IPS cannot be observed with zero-

dx.doi.org/10.1021/jp302545r | J. Phys. Chem. C 2012, 116, 13623−13628

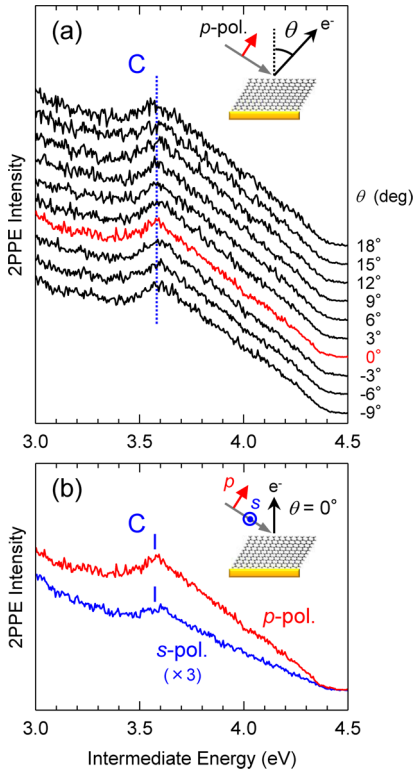

Figure 3. (a) AR-2PPE spectra for a C18-SAM/Au(111) surface measured with p-polarized light at a photon energy of 4.33 eV at RT in the region of the unoccupied C state. The photoemission angles are noted at the right-hand side, which were determined by rotating the sample. (b) Polarization dependence of the 2PPE spectra for a C18-SAM/Au(111) surface.

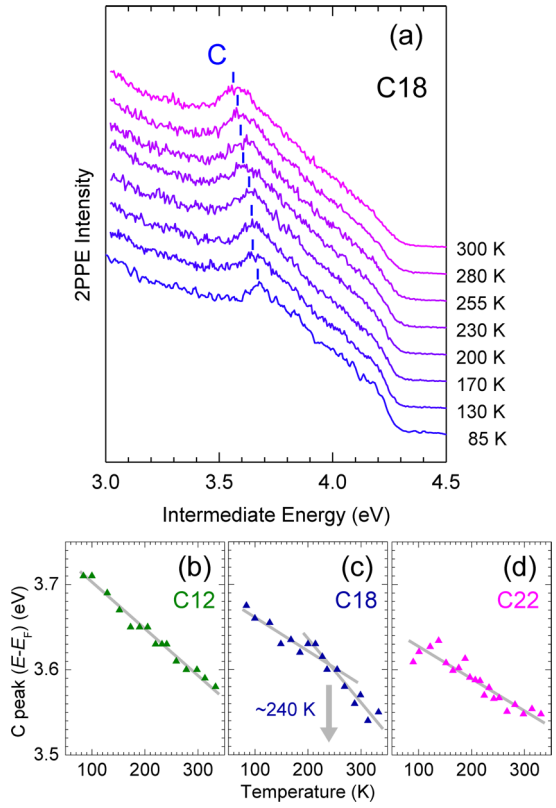

Figure 4. (a) Temperature dependence of 2PPE spectra for a C18-SAM/Au(111) surface measured with p-polarized light at a photon energy of 4.33 eV. The C state positions obtained from the 2PPE spectra were plotted against sample temperature for (b) the C12-SAM, (c) the C18-SAM, and (d) the C22-SAM/Au(111) substrate. The fitted lines indicate the energy shift rate of the C state with temperature; the rate changed at about 240 K for the C18-SAM [(c)].

delay 2PPE in this study is attributed to the finite rise time and the extremely long decay time of the IPS toward $k_{\parallel} = 0$. In other words, there is a small degree of overlapping of wave functions between the metal substrate and the IPS formed on a thick alkyl layer of SAM.

3.4. Temperature Dependence of the C State. As discussed in the preceding section, the C state is characterized by a localized state for Au−S bonds. Since the SAM exhibits several phases—crystal, rotator, and so on—depending on the temperature, we examined the temperature dependent properties of the electronic states using the localized character of the C state. Figure 4a shows the temperature dependence of 2PPE spectra for C18-SAM in the C state region. On increasing the substrate temperature from 85 to 330 K, the peak position of the C state was gradually shifted toward E_F. Similarly for C12- and C22-SAMs, the peak positions of each C state were also shifted toward E_F with a rise in temperature. Figure 4b−d shows the temperature dependence of the peak positions for C12-, C18-, and C22-SAMs. The shifts were approximately linear, but for C18-SAM (Figure 4c), the shift rate was changed around 240 K. Moreover, it is clearly shown that the shift rate of the C state decreases with increasing alkyl chain length.

The stabilization of the C state with temperature is attributed to the change in the SAM, and particularly to a change in the tilt angle of the alkyl chain. As reported previously in the IRAS experiments[45] and the molecular dynamic (MD) simulations,[46] the tilt angle depends on the temperature, being decreased with temperature as illustrated in Figure 5. The tilt angle decrement is a result of the dynamics that increase the freedom of motion

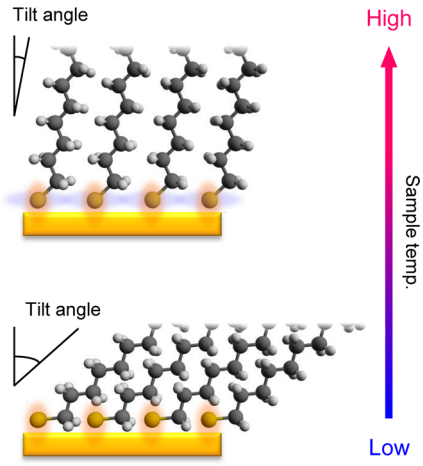

Figure 5. Schematic picture of the geometric structure of an alkanethiolate SAM on an Au(111) substrate. At low temperature (bottom), the tilt angle of the alkyl chain is large, and the interaction between neighboring sulfur atoms parallel to the surface would be small due to the interruption of the CH_2 group. On the other hand, at high temperature (top), the tilt angle becomes small and interaction between sulfur atoms would begin to occur.

for an individual alkyl chain, thereby maximizing the van der Waals interaction between alkyl chains.[47] The change in the tilt angle should affect the intermolecular interaction between neighboring S atoms parallel to the surface. At low temperature,

dx.doi.org/10.1021/jp302545r | J. Phys. Chem. C 2012, 116, 13623−13628

the interaction is quite small because of the spatial interruptions by the CH_2 group adjacent to the S atom, as shown in the bottom of Figure 5. With increasing temperature, the interruption is dissipated by standing up the alkyl chain, resulting in the stabilization of the C state.

Although the increased intermolecular interactions between such adsorbed molecules should lead to band dispersion, no significant band dispersion was observed in AR-2PPE; the C state did not exhibit dispersion at any temperatures in our experiment (not shown). No band dispersion could be ascribed to a relatively longer distance between neighboring S atoms. For our *n*-alkanethiolate SAM/Au(111) system, the distance between the neighboring S atoms is ~5 Å for the $(\sqrt{3} \times \sqrt{3})R30°$ or $c(4 \times 2)$ superstructure. For the methanethiolate/Ag(111) system,[48] in contrast, dispersive molecular-derived states were observed in saturated coverage, where the distance between S atoms is ~4.4 Å,[49,50] which is shorter than that on Au(111): the interaction between neighboring S atoms (~5 Å) would be too small to be detected as a significant band dispersion. It is noted that a nondispersive molecular-derived state was observed at low coverage of methanethiolate, because the methyl group lies on Ag(111) and disturbs the interaction between neighboring S atoms.[48]

In our study, the increase of intermolecular interaction was observed as the stabilization of the C state when the tilt angle of alkyl chains was changed with the substrate temperature. A similar stabilization has been reported for the thiophene/Au(111) system by White et al.[49] In the thiophene/Au(111) case, the unoccupied "S_u" state, which is very similar in energy position and spectral feature to the C state observed here, is gradually stabilized on increasing the thiophene coverage. A DFT calculation predicts that the phenyl plane tilted away from the surface plane with coverage, while the stabilization of "S_u" originates from the effect of charge-induced polarization of surrounding thiophene molecules.

As shown in Figure 4b–d, the energy shift rate of the C state with temperature became smaller as the alkyl chain of the SAM was lengthened. According to MD simulations,[46] the change of the tilt angle with respect to the surface normal is larger for a shorter alkyl chain (i.e., from 33° at 50 K to 17° at 300 K for C7-SAM and from 33° at 50 K to 29° at 300 K for C23-SAM). This is consistent with our observation; that is, the shift rate of the C state is less for a longer SAM. When the alkyl chain is lengthened, chain–chain interaction increases to form a more rigid alkyl comb, and thus, the temperature dependence of the tilt angle becomes smaller. The correlation between tilt angle variation and alkyl chain length was illustrated in Figure 6a and b.

For the C18-SAM, interestingly, the shift rate of the C state was changed at about 240 K. This change would be attributed to a thermodynamical conformation change in the SAM. In fact, according to the previous IRAS experiment for the C16-SAM/Au(111) system,[51] the alkyl chain starts to rotate near its end above 200 K, which is the so-called *all trans* to *gauche* transition. Above 280 K, furthermore, the chain tilt direction (Figure 3 in ref 46) becomes unlocked, and the alkyl chains behave as if they were in the liquid phase, as illustrated in Figure 6c.

In contrast, however, for the C12- and C22-SAMs, a change in the C state shift rate could not be observed at any temperatures. This implies that there are no significant phase transitions in the range of 85–330 K for both chain lengths of C12 and C22. Indeed, for the longer alkyl chain length, an *all trans* to *gauche* phase transition occurs at a higher temperature (i.e., at 300–400 K for C23-SAM in the MD simulation[46] and at ~350 K for C22-SAM by the IRAS measurement[52]) and the twist angle distribution is not noticeably changed.[46] Unfortunately, the temperature dependence of the C state shift cannot be measured above 330 K because the alkanethiolate molecules begin to gradually desorb above that temperature. For the shorter alkyl chain length, on the other hand, the ordering of SAM may be insufficient to cause an apparent shift change of the C state due to less interactions between the alkyl chains. In fact, it is known that the ordering of SAM is spoiled with decreasing alkyl chain length,[53] and then weaker interaction between alkyl chains in C12-SAM causes no rigid alkyl comb even at 85 K. The thermo-dynamical conformational change is therefore not prominent within the temperature range of 85–330 K, resulting in no slope change (Figure 4b).

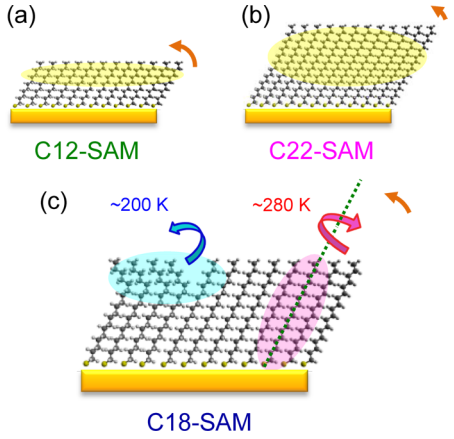

Figure 6. Schematic picture of the tilt angle variation difference between (a) short (C12) and (b) long (C22) alkanethiolate SAMs/Au(111) substrates. For the short alkyl chain, van der Waals interaction within alkyl chains (indicated by yellow shading) is so weak that the tilt angle changed markedly with temperature. For the long alkyl chain, on the other hand, the tilt angle is not changed much due to the strong alkyl chains interaction. (c) The phase transition of a C18-SAM/Au(111) substrate with temperature: an *all trans* to *gauche* transition occurs (blue shading) at above 200 K, and the chain tilt direction becomes unlocked (red shading) above 280 K.

4. CONCLUSIONS

We have investigated the electronic structures of C12-, C18-, and C22-alkanethiolate SAMs on an Au(111) substrate by 2PPE spectroscopy and observed three adsorption-induced electronic states (A, E_F +1.23 eV; B, E_F −2.83 eV; C, E_F +3.68 eV at 90 K). State C was characterized to be localized at an Au–S bond, and an energy shift toward the Fermi level was observed with increasing temperature. The C state shift was attributed to the change in the tilt angle of alkyl chains with temperature, which was emphasized by a shortening of the alkyl chain length. For the C18-SAM, furthermore, the rate of the C state shift was changed around 240 K, which might be caused by a phase transition of SAM; *all trans* to *gauche* transition above 200 K and unlocking of the chain tilt direction above 280 K. This study demonstrated that the photoemission spectroscopy can provide a powerful characterization tool for revealing the electronic states and surface properties formed by organic molecular layers on a substrate.

dx.doi.org/10.1021/jp302545r | J. Phys. Chem. C 2012, 116, 13623–13628

AUTHOR INFORMATION

Corresponding Author

*E-mail: nakajima@chem.keio.ac.jp. Fax: +81-45-566-1697.

Notes

The authors declare no competing financial interest.

ACKNOWLEDGMENTS

This work is partly supported by MEXT-Supported Program for the Strategic Research Foundation at Private Universities, 2009-2013.

REFERENCES

(1) Hickman, J. J.; Ofer, D.; Laibinis, P. E.; Whitesides, G. M.; Wrighton, M. S. *Science* **1991**, *252*, 688−691.
(2) Katz, E.; Lötzbeyer, T.; Schlereth, D. D.; Schuhmann, W.; Schmidt, H. L. *J. Electroanal. Chem.* **1994**, *373*, 189−200.
(3) Whelan, C. M.; Kinsella, M.; Carbonell, L.; Ho, H. M.; Maex, K. *Microelectron. Eng.* **2003**, *70*, 551−557.
(4) Xia, Y.; Whitesides, G. M. *Angew. Chem., Int. Ed.* **1998**, *37*, 550−575.
(5) Kumar, A.; Whitesides, G. M. *Science* **1994**, *263*, 60−62.
(6) Schreiber, F. *J. Phys.: Condens. Matter* **2004**, *16*, R881−R900.
(7) Schreiber, F. *Prog. Surf. Sci.* **2000**, *65*, 151−256.
(8) Love, J. C.; Estroff, L. A.; Kriebel, J. K.; Nuzzo, R. G.; Whitesides, G. M. *Chem. Rev.* **2005**, *105*, 1103−1169.
(9) Porter, M. D.; Bright, T. B.; Allara, D. L.; Chidsey, C. E. D. *J. Am. Chem. Soc.* **1987**, *109*, 3559−3568.
(10) Chailapakul, O.; Sun, L.; Xu, C.; Crooks, R. M. *J. Am. Chem. Soc.* **1993**, *115*, 12459−12467.
(11) Rodriguez, K. R.; Shah, S.; Williams, S. M.; Teeters-Kennedy, S.; Coe, J. V. *J. Chem. Phys.* **2004**, *121*, 8671−8675.
(12) Himmel, H. J.; Wöll, Ch.; Gerlach, R.; Polanski, G.; Rubahn, H. G. *Langmuir* **1997**, *13*, 602−605.
(13) Balzer, F.; Gerlach, R.; Polanski, G.; Rubahn, H. G. *Chem. Phys. Lett.* **1997**, *274*, 145−151.
(14) Camillone, N., III; Leung, T. Y. B.; Schwartz, P.; Eisenberger, P.; Scoles, G. *Langmuir* **1996**, *12*, 2737−2746.
(15) Kondoh, H.; Kodama, C.; Sumida, H.; Nozoye, H. *J. Chem. Phys.* **1999**, *111*, 1175−1184.
(16) Fukuma, T.; Ichii, T.; Kobayashi, K.; Yamada, H.; Matsushige, K. *J. Appl. Phys.* **2004**, *95*, 1222−1226.
(17) Xu, S.; Cruchon-Dupeyrat, S. J. N.; Garno, J. C.; Liu, G. Y.; Jennings, G. K.; Yong, T.; Laibinis, P. E. *J. Chem. Phys.* **1998**, *108*, 5002−5012.
(18) Poirier, G. E.; Pylant, E. D. *Science* **1996**, *272*, 1145−1148.
(19) Yamada, R.; Uosaki, K. *Langmuir* **1998**, *14*, 855−861.
(20) Poirier, G. E. *Langmuir* **1999**, *15*, 1167−1175.
(21) Sharma, M.; Komiyama, M.; Engstrom, J. R. *Langmuir* **2008**, *24*, 9937−9940.
(22) Lindstrom, C. D.; Muntwiler, M.; Zhu, X. Y. *J. Phys. Chem. B* **2005**, *109*, 21492−21495.
(23) Alloway, D. M.; Hofmann, M.; Smith, D. L.; Gruhn, N. E.; Graham, A. L.; Colorado, R.; Wysocki, V. H.; Lee, T. R.; Lee, P. A.; Armstrong, N. R. *J. Phys. Chem. B* **2003**, *107*, 11690−11699.
(24) Castner, D. G.; Hinds, K.; Grainger, D. W. *Langmuir* **1996**, *12*, 5083−5086.
(25) Steinmann, W. *Appl. Phys. A: Mater. Sci. Process.* **1989**, *49*, 365−377.
(26) Muntwiler, M.; Lindstrom, C. D.; Zhu, X.-Y. *J. Chem. Phys.* **2006**, *124*, 081104.
(27) Heinemann, N.; Leissner, T.; Grunau, J.; Rohwer, T.; Andreyev, O.; Bauer, M. *Chem. Phys.* **2011**, *382*, 1−4.
(28) Nakamura, T.; Miyajima, K.; Hirata, N.; Matsumoto, T.; Morikawa, Y.; Tada, H.; Nakajima, A. *Appl. Phys. A: Mater. Sci. Process.* **2010**, *98*, 735−743.
(29) Nakamura, T.; Hirata, N.; Sekino, Y.; Nagaoka, S.; Nakajima, A. *J. Phys. Chem. C* **2010**, *114*, 16270−16277.
(30) Shibuta, M.; Hirata, N.; Matsui, R.; Eguchi, T.; Nakajima, A. *J. Phys. Chem. Lett.* **2012**, *3*, 981−985.
(31) Lindstrom, C. D.; Muntwiler, M.; Zhu, X. Y. *J. Phys. Chem. B* **2007**, *111*, 6913−6920.
(32) Sugiyama, T.; Masuda, T.; Aida, M.; Ueno, N.; Munakata, T. *J. Electron Spectrosc. Relat. Phenom.* **2004**, *137−140*, 193−197.
(33) Chulkov, E. V.; Machado, M.; Silkin, V. M. *Vacuum* **2001**, *61*, 95−100.
(34) Lindstrom, C. D.; Quinn, D.; Zhu, X. Y. *J. Chem. Phys.* **2005**, *122*, 124714.
(35) Tegeder, P.; Hagen, S.; Leyssner, F.; Peters, M. V.; Hecht, S.; Klamroth, T.; Saalfrank, P.; Wolf, M. *Appl. Phys. A: Mater. Sci. Process.* **2007**, *88*, 465−472.
(36) Sonoda, Y.; Munakata, T. *Chem. Phys. Lett.* **2007**, *445*, 198−202.
(37) Yamada, T.; Shibuta, M.; Ami, Y.; Takano, Y.; Nonaka, A.; Miyakubo, K.; Munakata, T. *J. Phys. Chem. C* **2010**, *114*, 13334−13339.
(38) Zhang, L.; Goddard, W. A., III; Jiang, S. *J. Chem. Phys.* **2002**, *117*, 7342−7349.
(39) Toher, C.; Rungger, I.; Sanvito, S. *Phys. Rev. B* **2009**, *79*, 205427.
(40) Qi, Y.; Yaffe, O.; Tirosh, E.; Vilan, A.; Cahen, D.; Kahn, A. *Chem. Phys. Lett.* **2011**, *511*, 344−347.
(41) Seah, M. P.; Dench, W. A. *Surf. Interface Anal.* **1979**, *1*, 2−11.
(42) Clay, W. A.; Liu, Z.; Yang, W.; Fabbri, J. D.; Dahl, J. E.; Carlson, R. M. K.; Sun, Y.; Schreiner, P. R.; Fokin, A. A.; Tkachenko, B. A.; et al. *Nano Lett.* **2009**, *9*, 57−61.
(43) Kobayashi, K.; Horiuchi, T.; Yamada, H.; Matsushige, K. *Thin Solid Films* **1998**, *331*, 210−215.
(44) Szymanski, P.; Garrett-Roe, S.; Harris, C. B. *Prog. Surf. Sci.* **2005**, *78*, 1−39.
(45) Nagaoka, S.; Ikemoto, K.; Matsumoto, T.; Mitsui, M.; Nakajima, A. *J. Phys. Chem. C* **2008**, *112*, 6891−6899.
(46) Vemparala, S.; Karki, B. B.; Kalia, R. K.; Nakano, A.; Vashishta, P. *J. Chem. Phys.* **2004**, *121*, 4323−4330.
(47) Bhatia, R.; Garrison, B. J. *Langmuir* **1997**, *13*, 765−769.
(48) Miller, A. D.; Gaffney, K. J.; Liu, S. H.; Szymanski, P.; Garrett-Roe, S.; Wong, C. M.; Harris, C. B. *J. Phys. Chem. A* **2002**, *106*, 7636−7638.
(49) Zhou, J.; Yang, Y. X.; Liu, P.; Camillone, N., III; White, M. G. *J. Phys. Chem. C* **2010**, *114*, 13670−13677.
(50) Yu, M.; Driver, S. M.; Woodruff, D. P. *Langmuir* **2005**, *21*, 7285−7291.
(51) Dubois, L. H.; Nuzzo, R. G. *Annu. Rev. Phys. Chem.* **1992**, *43*, 437−463.
(52) Bensebaa, F.; Ellis, T. H.; Badia, A.; Lennox, R. B. *J. Vac. Sci. Technol. A* **1995**, *13*, 1331−1336.
(53) Bensebaa, F.; Ellis, T. H.; Badia, A.; Lennox, R. B. *Langmuir* **1998**, *14*, 2361−2367.